Experimental Evidence for Anisotropic Double-Gap Behavior in MgB_2

R. Cubitt and S. Levett
Institut Laue Langevin, Grenoble, France

S. L. Bud'ko, N. E. Anderson, and P. C. Canfield
Ames Laboratory and Department of Physics and Astronomy, Iowa State University, Ames, Iowa 50011
(Received 21 October 2002; published 17 April 2003)

The behavior of a type II superconductor in the presence of a magnetic field is governed by two characteristic length scales, the London penetration depth and the coherence length. We present magnetization measurements on MgB_2 powder showing an anisotropy in the upper critical field and hence the coherence length of 6. Using the technique of small angle neutron scattering we show that this anisotropy is not mirrored in the London penetration depth, which is almost isotropic. This result can be explained by the superconductivity residing in two distinct electronic bands of the material, only one of which is highly anisotropic.

DOI: 10.1103/PhysRevLett.90.157002 PACS numbers: 74.25.Ha, 74.25.Dw

Introduction.—MgB_2 is a relatively new discovery in the family of superconducting materials [1]. It has the highest critical temperature, T_c of 39 K for a simple binary compound. Intense technical interest stems from the fact that high critical currents can be obtained even with sintered powders and its ability to be formed into wires. In addition to the technological interest there are important questions concerning the superconducting mechanism that are still to be addressed. Measurements of the isotope effect [2] have shown that the attractive interaction forming superconducting electron pairs is photon mediated, as described by BCS theory. This theory has shown that crystal vibrations or phonons are responsible for an attractive interaction between electrons allowing them to pair up and condense into the superconducting state. Because of this interaction, a gap in the energetic states of the electrons opens up. An extension to this theory [3–6] involving multiple gaps has been applied in order to explain the relatively high T_c for a phonon-mediated superconductor. One consequence of the double-gap model (one of which is highly anisotropic) is that the anisotropy of two fundamental length scales can no longer be described by a single anisotropy parameter [5,6]. When a sample is cooled in an applied field H where $H_{c1} < H < H_{c2}$ quantized lines of flux thread the material sustained by a vortex of supercurrent. At the center of a vortex is a core of normal electrons, the characteristic size of which is the coherence length, ξ. The circulating current dies away from the core over the London magnetic penetration depth, λ. The upper critical field, H_{c2} above which the superconductivity is destroyed, is a function of ξ and the lower critical field, H_{c1} is largely determined by λ. Many measurements have shown a significant difference between H_{c2} measured with an applied field parallel to the *ab* plane to that crossing it, i.e., $\gamma_\xi = \xi_{ab}/\xi_c$. Low temperature values of γ_ξ originally clustered about 2 [7–11] with more recent values in the range 4–6 [12–16]. Ginsburg-Landau (GL) theory, applicable close to the critical temperature, predicts that any anisotropy in ξ must be reflected in λ, i.e., $\gamma_\xi = \gamma_\lambda$ where $\gamma_\lambda = \lambda_c/\lambda_{ab}$. The inequality of γ_λ and γ_ξ, below T_c, is exactly what has been predicted from models which take into account the electronic band structure in this material leading to the presence of two distinct energy gaps [3–6] one of which is highly anisotropic. These calculations show π-bonding orbitals having an essentially isotropic 3D nature and a small gap and anisotropic σ-orbital sheets with a gap approximately 4 times larger. It has been predicted [6] that at low temperatures $\gamma_\xi \sim 6$ and $\gamma_\lambda \sim 1.2$ with γ_ξ falling with increasing temperature and γ_λ rising to equal γ_ξ at a value of $\sim$2.5 at T_c. The values of γ_ξ experimentally evaluated from a number of measurements [12–17] are in agreement with the theoretical value of γ_ξ. We have followed the relatively simple method [14,17] of extracting γ_ξ from a powder by measuring the magnetization as a function of applied field. We also measure γ_λ on the same sample using the technique of small angle neutron scattering (SANS). A lattice of flux lines produces a modulating magnetic field, the amplitude of which is directly related to λ. The neutron, with its magnetic moment, is sensitive to this modulation and can coherently scatter from planes of flux lines resulting in Bragg peaks of detected neutron intensity. This is a direct measurement of the distance between flux-line planes, d. Here we deduce the anisotropy of λ by measuring the distribution of d. For the first time measurement of both γ_ξ and γ_λ have been made on the same sample and we find a remarkable agreement with the model based on the double-gap feature [6].

Experimental.—The sample used in this experiment was an unaligned powder enriched with ^{11}B to reduce neutron absorption. It was prepared from elemental Mg and isotopically enriched ^{11}B as described in Ref. [2]. Magnetization measurements of samples from the same source show a low temperature anisotropy of $\gamma_\xi \sim 6$ [14,17]. Using the same method we have measured γ_ξ

 © 2003 The American Physical Society

to be 6.7 ± 0.2 at 2 K with the highest upper critical field (with an applied field in the *ab* plane) of 16.1 ± 2 T. A thin layer of sample was sprinkled over an aluminium plate thinly coated in adhesive and the excess shaken off. The sample was then mounted in a cryostat, which was placed between hollow poles of an electromagnet allowing the neutron beam to pass through the sample to the detector with the applied field parallel to the beam. For neutrons of wavelength 10 Å a neutron beam is deflected by only $\sim 1°$ from a flux line density of 0.5 T. For this reason the small angle neutron scattering machine D22 at the Institut Laue Langevin was employed for these experiments. D22 allowed a 17.6 m collimation length resulting in a beam with a FWHM divergence of $0.174° \pm 2°$. A 1 m^2 multidetector with resolution 7.5 mm was placed 17.6 mm away from the sample. The incident neutron wavelength was 10 Å with a FWHM fractional lambda spread of 10%. With a powdered sample each grain contains a flux lattice of its own. The result is a ring of scattering, which was obtained by measuring the sample at 2 K, cooled in 0.5 T, and subtracting a background measured from the sample at 40 K as shown in Fig. 1. When measuring the scattering a beam stop was placed at the center of the detector to avoid the undeflected beam overloading the detector. The measurement of the incoming beam was realized by placing a calibrated attenuator in the beam and removing the beamstop. In principle we can measure the effective λ, which

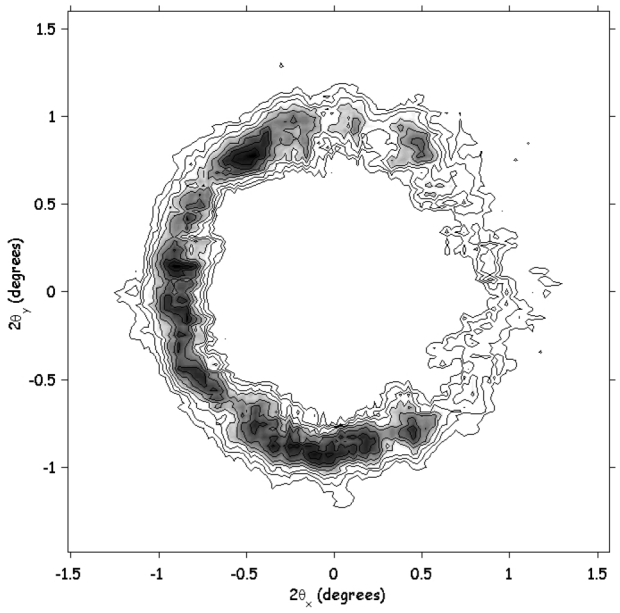

FIG. 1. The ring of scattering on the multidetector with the background subtracted. The contours are linear. The sample was field cooled in 0.5 T down to 2.0 K. The applied field and sample have been rotated 0.5° about a vertical axis, thus satisfying the Bragg condition on the left side of the ring. The data in Fig. 3 have been extracted from this picture by integrating the intensity as a function of deflected angle 2θ and normalizing by the area of each successive integration ring.

when coupled with γ_λ allows us to find both λ_{ab} and λ_c. However, in this work we concentrate on finding γ_λ and comparing it with γ_ξ. Our method for extracting γ_λ does not depend on the absolute values of λ_{ab} and λ_c, which only change the intensity of the scattering and not the spatial distribution.

Results.—Figure 1 shows the ring of intensity associated with the diffraction from the flux lattices in the powder after subtracting the background of 2 K and field cooled in 0.5 T. From the mean deflected angle of the scattering we can extract the mean separation of flux line planes from Braggs law

$$\lambda_n = 2d \sin(\theta), \tag{1}$$

where λ_n is the neutron wavelength, θ is half the deflected angle of the neutron mean, and d is the plane spacing of the flux lines. The mean plane spacing was found to be 620 ± 15 Å, which can be used to calculate the average flux density in the bulk assuming a square lattice (0.53 T) or a triangular lattice (0.46 T). Clearly the flux line density in the bulk cannot exceed the applied field of 0.5 T so we conclude that the flux lattice is triangular as expected with hexagonal crystal symmetry. In a randomly oriented powder where ψ is the angle between the c axis of a grain and the applied field we sample grains with a statistical weighting of $\sin\psi$. Anisotropy of λ results in currents flowing in an elliptical form about a flux line axis when the current is forced to cross the *ab* plane, i.e., $\psi > 0$. The spacing between flux line planes adjusts itself to equalize the repulsion from its neighbors and the result is an elliptical locus of scattering from a single grain of eccentricity $1/(\cos^2\psi + \sin^2\psi/\gamma_\lambda^2)^{1/2}$ [18]. Clearly when $\psi = 0$ $(B//c)$ the lattice is undistorted, independently of the value of γ_λ. A distorted flux lattice in a randomly oriented crystal and the resultant scattering pattern is shown in Fig. 2. The angle α defines the orientation of the flux lattice relative to the minor axis of the ellipse as defined in Ref. [18]. This was demonstrated [19] with a single crystal of $YBa_2Cu_3O_7$ where the anisotropy of λ was mirrored in the elliptical arrangement of Bragg peaks.

Clearly from Eq. (1) the presence of anisotropy, amplified by the geometrical $\sin\psi$ factor, will result in a distribution of d spacings and hence broaden the width of the ring as seen in Fig. 1. Figure 3 shows the measured intensity as a function of scattered angle of the beam. This is clearly broader than the case where $\gamma_\lambda = 1$ which represents the instrument resolution. We model the effects of this broadening by summing the flux lattice contributions to the scattering from each grain in the sample [18]. Assuming the flux lattice orientation about the field direction is pinned to a particular crystal axis in a grain we must sum over all possible flux lattice structures within a given ellipse defined by ψ and γ_λ over the ranges $\alpha = 0\text{-}\pi/3$ and $\psi = 0\text{-}\pi/2$ weighting by $\sin\psi$. This range of α entirely fills each ellipse with intensity. The result must be summed over all azimuthal angles, β on

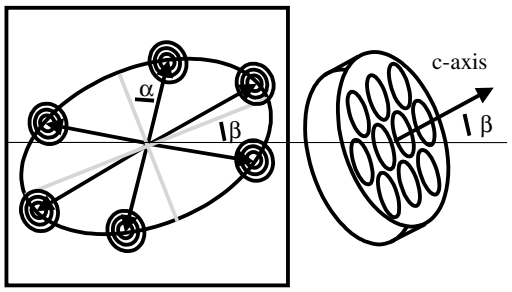

FIG. 2. The left shows the scattering on the detector expected from a single grain when $\gamma_\lambda > 1$ and $\psi > 0$ where ψ is the angle between the c axis of the crystal and the applied field normal to the page. The right shows a crystal at an arbitrary orientation showing the vortices of supercurrent around each flux line. The angle β is the projected angle of the c axis (and major axis of the ellipse) to the horizontal. The model involves summing over the scattering patterns for $\psi = 0$ to $\pi/2$, weighting by $\sin\psi$, summing over all α from 0 to $\pi/3$ (or setting $\alpha = 0$) and then integrating the result over all azimuthal angles β. With the eccentricity of each ellipse equal to $1/(\cos^2\psi + \sin^2\psi/\gamma_\lambda^2)^{1/2}$, the result is an increasing broadening of the intensity as a function of 2θ with increasing γ_λ. The gray lines show the major and minor axes of the ellipse.

the "detector" as each ellipse can have any orientation. Each lattice constructed consisted of six Bragg peaks of FWHM 0.197°. This width represents the instrumental resolution coming from the wavelength spread and the divergence of the incoming beam [20]. Campbell [18] has shown that the orientation $\alpha = 0$ is energetically favorable so we model this case in addition to the random orientation corresponding to a preferential crystal direction in the ab plane for a flux line plane. We use a χ^2 criterion to find the value of γ_λ which gives the best fit to the data. For the first case with $\alpha = 0$-$\pi/3$ we obtain $\gamma_\lambda = 1.32 \pm 1$ with $\chi^2 = 1.12$ and for the second with $\alpha = 0$ we have $\gamma_\lambda = 1.28 \pm 1$ with $\chi^2 = 1.28$. The values of χ^2 are so close we cannot distinguish between these two cases but both give similar values for γ_λ only because γ_λ is close to 1. Figure 3 also shows the intensity distribution for γ_λ set to $\gamma_\xi = 6.7$ for the two orientation cases, both of which are inconsistent with the data. Figure 4 shows the data derived here along with the theoretical predictions for $\gamma_\lambda(T)$ and $\gamma_\xi(T)$.

The values for γ_λ were derived assuming that the only sources of the scattered intensity width came from the instrument resolution and the anisotropy in λ. The presence of other sources of d-spacing variation leads to an overestimation of γ_λ so we can take the value of 1.32 as an upper bound. We did, however, take care to avoid multiple scattering effects by reducing the mass of sample in the beam such that we were in a regime where the width of the scattered intensity was independent of sample quantity. The finite size of the flux lattices confined in each grain does not lead to broadening as we estimate the transverse coherence of the neutron beam (0.3 μm) to be smaller than the lower bound of grain sizes seen by electron microscopy. Other possible small sources of broadening involve considerations of the perfection of the flux lattice formed in each grain. We do not consider these cases as the principle result of this study is the demonstration of the inequality of γ_λ and γ_ξ.

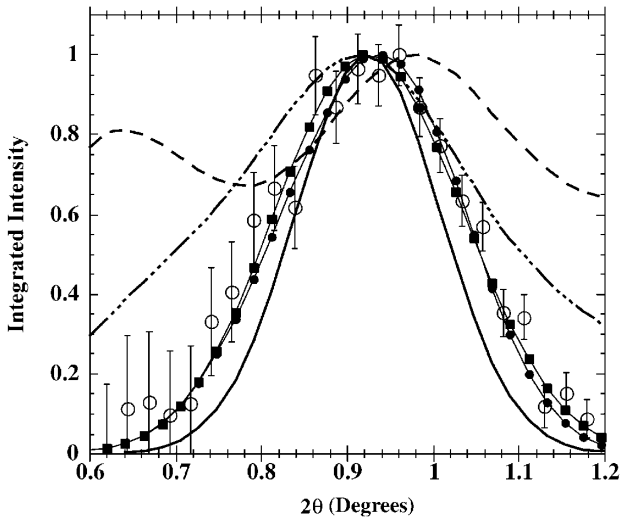

FIG. 3. The variation of scattering as a function of deflected angle of the beam integrated 360° about the undeflected beam axis. The dashed line and the solid squares are the models with $\alpha = 0°$–$60°$ for $\gamma_\lambda = 6.70$ and 1.32, respectively. The dot-dashed line and the solid circles are the models with $\alpha = 0°$ for $\gamma_\lambda = 6.70$ and 1.28, respectively. The solid line is the model for $\gamma_\lambda = 1$ (the width is the instrument resolution) and the open circles are the data. Clearly the value $\gamma_\xi = 6.7$, taken from magnetization measurements does not correspond to the data with either of the possible orientations.

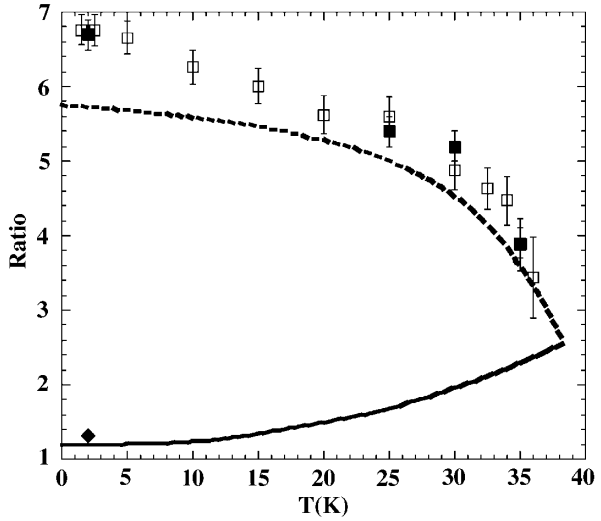

FIG. 4. The open squares show γ_ξ from Ref. [14] measured with a sample from the same source. The solid squares are γ_ξ measured on this sample using the same magnetization method. The dotted and solid lines show the theoretical predictions for γ_ξ and γ_λ in clean MgB_2 with a gap ratio of 4 [5,6]. The solid diamond is the upper limit for γ_λ derived from the neutron measurements described here.

Conclusions.—We have made accurate measurements of an upper limit of γ_λ and found that compared to the anisotropy in ξ (derived from magnetization measurements) it is almost isotropic as predicted by a double-gap model [5,6]. The two-gap model predicts an almost isotropic variation of λ as this depends only on the total density of superconducting carriers and the effective carrier mass anisotropy, not on the anisotropy of the gap for clean superconductors [5,6]. The gap anisotropy, principally coming from the σ bands with the larger gap only has a strong effect on ξ. It should be noted that a double gap without associated anisotropy in one or both of the gaps would not show the different anisotropies we have observed. Impurity scattering tends to blur out the double-gap structure so only cleaner samples are likely to show high values of γ_ξ, which could explain the wide variation in measured values. We see a remarkable agreement between both anisotropy values and the theoretical predictions. The consequence of this result for applications are double edged. For sintered polycrystalline samples we would like to be able to pass the highest current density possible. The high value of γ_ξ means we suffer a relatively low value of H_{c2} when the applied field is parallel to the c axis (~ 2.5 T) so an increasing fraction of the grains are turned normal at applied fields greater than this. However, the propensity of the flux lattice to melt [21], become mobile, and induce electrical resistance when passing a current is reduced with an almost isotropic λ.

The authors are grateful to V. G. Kogan and C. Dewhurst for helpful discussions. Work at Ames Laboratory was supported by the Director for Energy Research, Office of Basic Science, U.S. Department of Energy.

[1] J. Nagamatsu, N. Nakagawa, T. Muranaka, Y. Zenitani, and J. Akimitsu, Nature (London) **410**, 63 (2001).
[2] S. L. Bud'ko, G. Lapertot, C. Petrovic, C. E. Cunningham, N. Anderson, and P. C. Canfield, Phys. Rev. Lett. **86**, 1877 (2001).
[3] A. Y. Liu, I. I. Mazin, and J. Kortus, Phys. Rev. Lett. **87**, 087005 (2002).
[4] H. J. Choi, D. Roundy, H. Sun, M. L. Cohen, and S. G. Louie, Nature (London) **418**, 758 (2002).
[5] V. G. Kogan, Phys. Rev. B **66**, 020509 (2002).
[6] P. Miranovic, K. Machida, and V. G. Kogan, J. Phys. Soc. Jpn. **72**, 221 (2003).
[7] A. K. Pradhan, Z. X. Shi, M. Tokunaga, T. Tamegai, Y. Takano, K. Togano, H. Kito, and H. Ihara, Phys. Rev. B **64**, 212509 (2001).
[8] O. F. de Lima, C. A. Cardoso, R. A. Ribeiro, M. A. Avila, and A. A. Coelho, Phys. Rev. B **64**, 144517 (2001).
[9] M. Xu, H. Kitazawa, Y. Takano, J. Ye, K. Nishida, H. Abe, A. Matsushita, N. Tsujii, and G. Kido, Appl. Phys. Lett. **79**, 2779 (2001).
[10] O. F. de Lima, R. A. Ribeiro, M. A. Avila, C. A. Cardoso, and A. A. Coelho, Phys. Rev. Lett. **86**, 5974 (2001).
[11] K. H. P. Kim, J. H. Choi, C. U. Jung, P. Chowdhury, H. S. Lee, M. S. Park, H. J. Kim, J. Y. Kim, Z. Du, E. M. Choi, M. S. Kim, W. N. Kang, S. I. Lee, G. Y. Sung, and J. Y. Lee, Phys. Rev. B **65**, 100510 (2002).
[12] G. Papavassiliou, M. Pissas, M. Fardis, M. Karayanni, and C. Christides, Phys. Rev. B **65**, 012510 (2001).
[13] F. Simon, A. Janossy, T. Feher, F. Muranyi, S. Garaj, L. Forro, C. Petrovic, S. L. Bud'ko, G. Lapertot, V. G. Kogan, and P. C. Canfield, Phys. Rev. Lett. **87**, 047002 (2001).
[14] S. L. Bud'ko, and P. C. Canfield, Phys. Rev. B **65**, 212501 (2002).
[15] A. V. Sologubenko, J. Jun, S. M. Kazakov, J. Karpinski, and H. R. Ott, Phys. Rev. B **65**, 180505 (2002).
[16] M. Angst, Puzniak, A. Wisniewski, J. Jun, S. M. Kazakov, J. Karpinski, J. Roos, and H. Keller, Phys. Rev. Lett. **88**, 167004 (2002).
[17] S. L. Bud'ko, V. G. Kogan, and P. C. Canfield, Phys. Rev. B **64**, 180506 (2001).
[18] L. J. Campbell, M. M. Doria, and V. G. Kogan, Phys. Rev. B **38**, 2439 (1988).
[19] M. Yethiraj, H. A. Mook, G. D. Wignall, R. Cubitt, E. M. Forgan, S. L. Lee, D. M. Paul, and T. Armstrong, Phys. Rev. Lett. **71**, 3019 (1993).
[20] R. Cubitt, E. M. Forgan, D. McK. Paul, S. L. Lee, J. S. Abell, H. Mook, and P. A. Timmins, Physica (Amsterdam) **180B & 181B**, 377 (1992).
[21] R. Cubitt, E. M. Forgan, G. Yang, S. L. Lee, D. McK Paul, H. A. Mook, M. Yethiraj, P. H. Kes, T. W. Li, A. A. Menovsky, Z. Tarnawski, and K. Mortensen, Nature (London) **365**, 407 (1993).